

π_0 Mass Enhancement for the Backward Reaction $\pi^-p \rightarrow p(\pi_0)^-$ in a Double-Regge-Pole Model*

CHIA-CHANG SHIH† AND BING-LIN YOUNG

Brookhaven National Laboratory, Upton, New York 11973

(Received 14 October 1969)

Using a double-Regge-pole model, we investigate the π_0 mass enhancement in the backward reaction $\pi^-p \rightarrow p(\pi_0)^-$. Broad peaks occur in this model near the A_1 mass. They are found to persist under a wide range of Regge-parameter values. Similar features also hold for the forward reaction cases. We conclude that the mass enhancement comes from the interplay of the phase-space kinematics and the peripheral nature of the Regge amplitude; the specific intercept and slope values of the trajectories are not very crucial. On the basis of our findings, we discuss the implications of the duality principle, isospin complications, and the practical problem of how to describe the A_1 .

I. INTRODUCTION

IN a recent high-energy backward scattering experiment $\pi^-p \rightarrow pX^-$,¹ X^- mass enhancements in the "A" region have been observed. With the present statistics, the data for " A_1 " already indicate very interesting features similar to those of its production in the forward direction.²

Previous studies have suggested that the forward production of A_1 can be explained by the Drell-Hiida-Deck (DHD) mechanism.³ A more sophisticated model with double-Regge-pole (DR) exchanges also fitted the experimental data well.⁴ These models, as applied to the (forward) reaction $\pi p \rightarrow \pi p p$, containing diffraction-dissociation scattering, produce peripherally an enhancement of the π_0 system in the A_1 region. As to whether A_1 is a genuine resonance or merely a kinematical enhancement has therefore been a puzzle for some time.⁵ By extending the duality principle to multiparticle reactions, a resolution has been advanced.⁶ Accordingly, the peripheral approximation to

an amplitude represents on the average the resonances, although it does not contain energy poles in a given subchannel of the final state. The Deck effect can, therefore, be interpreted so as to predict the existence of A_1 .

However, these DHD and DR models involve a virtual diffraction vertex; they do not lead us directly to an understanding of similar processes without vacuum-quantum number exchanges. On the other hand, as mentioned, the A_1 has indeed been observed in the backward direction¹ and many other places.⁷ In the backward case, it not only has a narrow width (~ 100 MeV), but also is more peripheral than π^- , ρ^- , A_2^- , etc. observed in the same process. The latter feature is usually associated with the DHD effect.^{3,4,8}

This immediately suggests to us the question of whether these properties can also be understood in terms of a similar type of calculation using baryon exchanges.⁹ In this article, we shall apply the DR model to the backward reaction $\pi^-p \rightarrow p(\pi_0)^-$ and compare it with the experimental data. This enables us to examine possible distinctions between the present case and that of the general forward A_1 productions. We may also gain in our model some insight of how duality comes into play in the backward production processes.¹⁰

* Work performed under the auspices of the U.S. Atomic Energy Commission.

† Present address: Department of Physics, Carnegie-Mellon University, Pittsburgh, Pa. 15213.

¹ E. W. Anderson, E. J. Bleser, H. R. Blieden, G. B. Collins, D. Garelick, J. Menes, F. Turkot, D. Birnbaum, R. M. Edelstein, N. C. Hien, T. J. McMahon, J. Mucci, and J. Russ, *Phys. Rev. Letters* **22**, 1390 (1969).

² See, for example, the review by I. Butterworth, in *Proceedings of the International Conference on Elementary Particles, Heidelberg, 1967*, edited by H. Filthuth (North-Holland, Amsterdam, 1968), p. 12. See also M. L. Ioffredo, G. W. Brandenburg, A. E. Brenner, B. Eisenstein, L. Eisenstein, W. H. Johnson, Jr., J. K. Kim, M. E. Law, B. M. Salzberg, J. H. Scharenguivel, L. K. Sistrone, and J. Szymanski, *Phys. Rev. Letters* **21**, 1212 (1968).

³ S. D. Drell and K. Hiida, *Phys. Rev. Letters* **7**, 199 (1961); R. T. Deck, *ibid.* **13**, 169 (1964); U. Maor and T. A. O'Halloran, *Phys. Letters* **15**, 281 (1965); U. Maor, *Ann. Phys. (N.Y.)* **41**, 456 (1967); L. Stodolsky, *Phys. Rev. Letters* **18**, 973 (1967); M. Ross and Y. Yam, *ibid.* **19**, 546 (1967).

⁴ E. L. Berger, *Phys. Rev.* **166**, 1525 (1968); **179**, 1567 (1969).

⁵ For recent discussions, see R. T. Poe, B. R. Desai, A. Kernan, and H. K. Shepard, *Phys. Rev. Letters* **22**, 551 (1969); A. S. Goldhaber, C. Joachain, H. J. Lubatti, and J. J. Veillet, *ibid.* **22**, 802 (1969).

⁶ G. F. Chew and A. Pignotti, *Phys. Rev. Letters* **20**, 1078 (1968).

⁷ A. M. Cnops, P. V. C. Hough, F. R. Huson, I. R. Kenyon, J. M. Scarr, I. O. Skillicorn, H. O. Cohn, R. D. McCulloch, W. H. Bugg, G. T. Condo, and M. M. Nussbaum, *Phys. Rev. Letters* **21**, 1609 (1968); I. R. Kenyon, J. B. Kinson, J. M. Scarr, I. O. Skillicorn, H. O. Cohn, R. D. McCulloch, W. M. Bugg, G. T. Condo, and M. M. Nussbaum, *ibid.* **23**, 146 (1969); D. J. Crennel, U. Kaishon, K. W. Lai, J. S. O'Neill, and J. M. Scarr, *ibid.* **22**, 1327 (1969); J. V. Allaby, F. Binon, A. N. Diddens, P. Duttell, A. Klovning, R. Mennier, J. P. Peigneux, E. J. Sachharadis, K. Schlüppmann, M. Spighele, J. P. Stroot, A. M. Thorndike, and A. M. Wetherell, *Phys. Letters* **29B**, 198 (1969). A_1 has also been observed in many reactions involving four or more final particles.

⁸ B. Y. Oh and W. D. Walker, *Phys. Letters* **28B**, 564 (1969).

⁹ A similar type of charge-exchange Deck model for the doubly charged final state ($K^*\pi^+$) has been studied by F. Bomse and E. J. Moses, *Phys. Rev.* **176**, 2163 (1968).

¹⁰ Two-body reactions which are dominated by baryon Regge-pole exchanges have been reviewed extensively by V. Barger, University of Wisconsin Report No. COO-881-216 (unpublished).

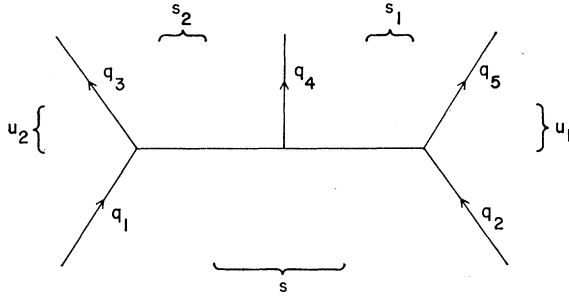


FIG. 1. Kinematic assignment and Regge behavior for reaction (1).

In Sec. II, we review very briefly the kinematics, and write down the production amplitudes in the model of double Regge poles. In Sec. III, we present the Chew-Low plots against an appropriate set of variables and comment on the experimental situation. Isospin complications and "partial-wave" projections are also examined. A comparison of the forward (with or without diffraction vertices) and backward A_1 production composes Sec. IV. In Sec. V we make several remarks and summarize our results.

II. FIVE-BODY KINEMATICS AND DOUBLE-REGGE-POLE AMPLITUDES

To establish the notation, let us denote the process to be considered by

$$q_1 + q_2 \rightarrow q_3 + q_4 + q_5, \tag{1}$$

where q_i denotes the i th particle as well as its four-momentum. A double-baryon Regge-pole amplitude for (1) can then be represented as in Fig. 1. Following the usual convention, we can express the amplitude of (1) in terms of the five independent invariants

$$\begin{aligned} s &\equiv (q_1 + q_2)^2, \\ s_1 &\equiv (q_4 + q_5)^2 \equiv w^2, \\ s_2 &\equiv (q_3 + q_4)^2, \\ u_1 &\equiv (q_2 - q_5)^2, \\ u_2 &\equiv (q_1 - q_3)^2. \end{aligned} \tag{2}$$

The differential cross section for (1) is given by

$$d\sigma_3 = \frac{1}{\prod (2s_i + 1)} \frac{(2\pi)^{-5}}{2\lambda^{1/2}(s, m_1^2, m_2^2)} \sum_{s_i, s_f} |\mathcal{F}_3|^2 d\Phi_3, \tag{3}$$

where $d\Phi_3$ is the three-body phase space,¹¹ s_i (s_f) are the spins of the initial (final) particles which are averaged (summed) over, and $2\lambda^{1/2}$ is the incoming flux. In terms of the invariant variables, we have

$$d\sigma_3 = \lambda^{-1/2}(s, m_1^2, m_2^2) \int \dots \int |M_3|^2 \times [ds_2 ds_1 du_2 du_1 / (-\Delta_4)^{1/2}], \tag{4}$$

where $\Delta_4 = \Delta_4(q_1, q_2, q_4, q_5)$ is a well-known phase-space factor. The explicit form of Δ_4 and its general properties can be found in the literature.¹¹ M_3 denotes the effective amplitude obtained from \mathcal{F}_3 after carrying out the spin averaging and summation. To simplify the calculation we shall approximate M_3 , as usual, by

$$M_3 = \sum_j f_{2i}(u_2) \xi_i(u_2) (s_2/s_{20})^{\alpha_{2i}(u_2)} \times g_{ij}(u_2, u_1, \omega) (s_1/s_{10})^{\alpha_{1j}(u_1)} \xi_j(u_1) f_{1j}(u_1),$$

$$\xi_i = \frac{1 \pm \exp[i\pi(\alpha_i - \frac{1}{2})]}{\sin\pi(\alpha_i - \frac{1}{2})}, \tag{5}$$

where ω is the Toller angle, and f_{2i} , f_{1j} , and g_{ij} are residue functions associated with Regge trajectories i and j .¹² Since we have anticipated the situation that there is only one leading Regge pole, i , to be exchanged in u_2 , we do not sum over i . In the spirit of the multiperipheral model,¹³ we shall assume that the g_{ij} 's depend weakly¹⁴ on ω and are separable in u_1 and u_2 , i.e.,

$$g_{ij}(u_1, u_2, \omega) \simeq \text{const } f_{2i}'(u_2) f_{1j}'(u_1). \tag{6}$$

Let us consider a quantity $R(s, s_1, u_2)$, which is defined as the ratio of (3) to the differential cross section of an associated two-body reaction of the same total energy s and the momentum transfer u_2 . This two-body reaction is obtained from (2) by deleting q_2 and q_5 and putting α_1 on the mass shell, i.e.,

$$\alpha_1(\text{on shell}) + q_1 \rightarrow q_3 + q_4, \tag{7}$$

as illustrated in Fig. 2. Again by ignoring the spin complications, a similar expression of the differential cross section for (7) can be written as

$$d\sigma_2 = \lambda^{-1/2}(s, m_1^2, m_{\alpha_1}^2) |M_2|^2 du_2,$$

where $m_{\alpha_1}^2$ is the proper physical mass of α_1 , and

$$M_2 = \sum_i g_{2i}(u_2) (s/s_{20})^{\alpha_{2i}(u_2)} \xi_i g_{2i}'(u_2). \tag{8}$$

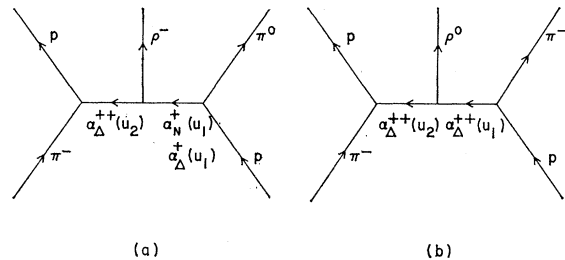


FIG. 2. Diagram for the reactions (a) $\pi^- + p \rightarrow p + \rho^- + \pi^0$ and (b) $\pi^- + p \rightarrow p + \rho^0 + \pi^-$.

¹¹ See, for example, H.-M. Chan, K. Kajantie, and G. Ranft, Nuovo Cimento 49, 157 (1967); K. Kajantie and P. Lindblom, Phys. Rev. 175, 2203 (1968).

¹² I. T. Drummond, Phys. Rev. 176, 2003 (1968). We consider only the leading trajectories allowed in each channel.

¹³ G. F. Chew and A. Pignotti, Phys. Rev. 176, 2112 (1968).

¹⁴ R. A. Morrow, Phys. Rev. 176, 2147 (1968).

In the present case, we shall consider a particular reaction of (7), i.e.,



Since the above reaction is dominated by a Δ trajectory, we have

$$d\sigma_3(s, s_1, u_2)/ds_1 du_2 \equiv [d\sigma_2(s, u_2)/du_2] R(s, s_1, u_2), \quad (10)$$

where

$$R(s, s_1, u_2) = \int \int [ds_2 du_1 / (-\Delta_4)^{1/2} |M|^2], \quad (11)$$

$$M = \sum_j (s_2/s)^{\alpha_{2i}(u_2)} (s_1/s_{10})^{\alpha_{1j}(u_1)} \times \xi_{1j}(u_1) \beta_j(u_1) \beta_2(u_2) N_j,$$

$$\beta_j(u_1) = f_{1j}(u_1) f_{1j}'(u_1),$$

$$\beta_2(u_2) = f_{2i}(u_2) f_{2i}'(u_2) (g_\Delta(u_2) g_\Delta'(u_2))^{-1}. \quad (12)$$

The quantity N_j serves as a normalization constant such that we can define $\beta_j(0) = \beta_2(0) = 1$. In the following, we shall work with $R(s, s_1, u_2)$, which provides us with a measure of (1) relative to the associated two-body reaction (9). We shall see later that $R(s, s_1, u_2)$ is almost independent of s .¹⁵ Let us emphasize that in defining R , Eq. (10), we have departed from the conventional treatment in which the energy variable of the associated two-body reaction (7), and therefore (8), is s_2 . (See, for example, Ref. 16.) Our purpose is not to isolate an off-shell two-body reaction from the three-body reaction as is usually done, e.g., in the one-particle-exchange model. Here, R is a device which enables us to compare directly the three-body and the associated two-body reactions at the same energy. As we shall discuss later, this is to compare the A_1 production with that of ρ . Since for fixed s and u_2 , $d\sigma_2/du_2$ is constant, R therefore gives all the information of $d\sigma_3/ds_1 du_2$ for given values of these fixed variables.

Before evaluating (11), let us remark that in writing down (5), there is always an ambiguity concerning the detailed form of the energy variables to be adopted in the low-energy region (down to the threshold value of s_1). In the formulation of the multiperipheral model, the s_1 dependence comes from⁴

$$s_1 \cdots = s_1 - u_2 - m_2^2 + u_1^{-1} (m_3^2 - m_2^2 - u_1) (m_4^2 - u_1 - u_2). \quad (13)$$

It has a pole at $u_1 = 0$, which is in the physical region [see Fig. 3(a)]. Although the singular part is to be canceled by daughter trajectories, the finite part remains ambiguous. We shall here restrict ourselves to the simplest expression for s_1 , and similarly for s_2 [as is used in (5) and (8)]. We shall comment on some other choices later on.

¹⁵ G. F. Chew, C. Detar, and A. Pignotti, Phys. Rev. **180**, 1577 (1969).

¹⁶ E. Ferrari and F. Selleri, Nuovo Cimento Suppl. **24**, 453 (1962).

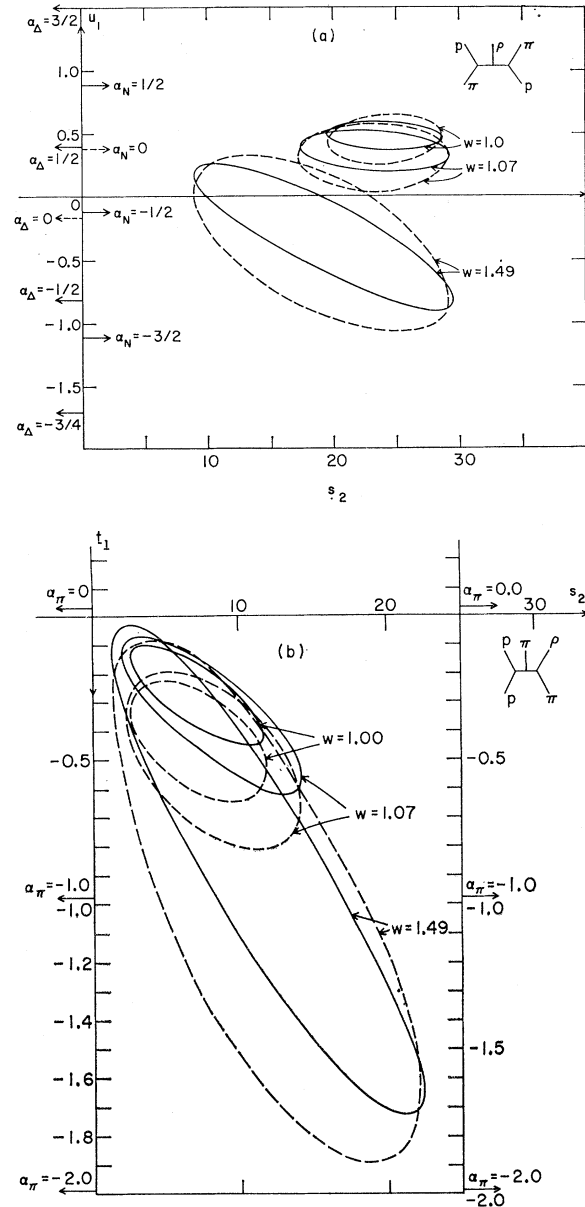


FIG. 3. (a) Phase-space boundaries in (s_2, u_1) (in units of GeV^2) for different values of (s_1, u_2) for the backward reaction $\pi + p \rightarrow p + \rho + \pi$. (b) Phase-space boundaries in (s_2, t_1) for different values of (s_1, t_2) for the forward reaction $\pi + p \rightarrow p + \rho + \pi + p$. (Here the momentum transfers are denoted by t_1 and t_2 , respectively.) The values of u_1 (t_1) where the trajectory functions [given by (17) and $\alpha_\pi(t) = t - m_\pi^2$] take integer or half-integer values are indicated on the u_1 (t_1) axis. The solid and dashed curves are for u_2 (t_2) = -0.11 and -0.31 , respectively. $w = s_1^{1/2}$ is in units of GeV .

To illustrate the variation of the integration region of (11) under the changes of s_1 and u_2 , we plot in Fig. 3 the phase-space boundaries of (s_2, u_1) at $s = 31$ GeV^2 for several values of s_1 and u_2 . For comparison we also plot the analogous region for the forward scattering case.

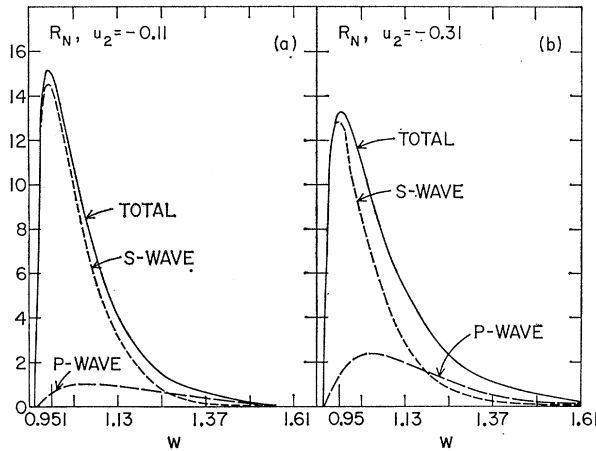


FIG. 4. The R_N distribution with parameters listed in (17). (a) $u_2 = -0.11$ GeV²; (b) $u_2 = -0.31$ GeV².

III. GENERAL FEATURES OF MASS ENHANCEMENT IN FINAL πp SYSTEM

Let us consider specific cases of (1),

$$\pi^- + p \rightarrow p + \begin{cases} \rho^- + \pi^0 \\ \rho^0 + \pi^- \end{cases}, \quad (14)$$

which are illustrated in Figs. 2(a) and 2(b), respectively. The symbols are self-explanatory. For the diagram in Fig. 2(a), the trajectory on the left must be $\alpha_{\Delta}^{++}(u_2)$; on the right-hand side, two interfering trajectories $\alpha_{\Delta}^{+}(u_1)$ and $\alpha_N^{+}(u_1)$ are allowed. Because of our lack of knowledge concerning the center vertex and the spin complications, it is difficult to treat the interference effect rigorously; a more detailed understanding of their structure is needed. Nevertheless, in order to exhibit the essential features, we shall examine this effect in terms of their (individually) spin-averaged amplitudes. For the diagram of Fig. 2(b), only $\alpha_{\Delta}^{++}(u_2)$ and $\alpha_{\Delta}^{+}(u_1)$ dominate the amplitude.

Diagrams obtained from Fig. 2 by interchanging ρ and π are omitted. They are expected to be small.¹⁷ Furthermore, their main contributions come from a phase-space region different from that of Fig. 2, and therefore do not produce a strong interference effect.¹⁸

¹⁷ For diagrams obtained from 2(a) and 2(b) with ρ and π interchanged, the phase space in u_1 is farther away from the elementary pole positions of $\alpha_i(u_1)$ as compared with those of the diagrams of Figs. 2(a) and 2(b). With comparable coupling strengths for both cases, the contributions of the omitted diagrams will be smaller than those of Figs. 2(a) and 2(b). Detailed calculations (not presented in the text) showed that their distribution function $R(s, s_1, u_2)$ has also very different characteristics from those of Figs. 2(a) and 2(b) and is probably not responsible for the observed A_1 .

¹⁸ The diagram with the final proton going out from the central vertex is not enhanced at small values of s_i and $|u_2|$. See L. Caneschi and A. Pignotti, Phys. Rev. Letters 22, 1219 (1969).

In the numerical calculations, we parametrize the trajectories as

$$\begin{aligned} \alpha_N(u) &= \alpha_N^{(0)} + \alpha_N^{(2)}u, \\ \alpha_{\Delta}(u) &= \alpha_{\Delta}^{(0)} + \alpha_{\Delta}^{(2)}u. \end{aligned} \quad (15)$$

Our results are not very sensitive to the exact values of these parameters. As for the center vertex, the parametrization depends upon the choices of the ghost-eliminating mechanisms for the individual trajectories. For example, with the choice of nonsense wrong-signature zeros at $\alpha_N = -\frac{1}{2}$ and $\alpha_{\Delta} = -\frac{3}{2}$, we put

$$\begin{aligned} \beta_N(u_1) &= [\alpha_N(u_1) + \frac{1}{2}] [\alpha_N(u_1) + \frac{3}{2}] \exp(\gamma_N u_1), \\ \beta_{\Delta}(u_1) &= [\alpha_{\Delta}(u_1) + \frac{1}{2}] [\alpha_{\Delta}(u_1) + \frac{3}{2}] \exp(\gamma_{\Delta} u_1). \end{aligned} \quad (16)$$

If the residue functions choose finite values at specific nonsense wrong-signature points, the corresponding zero factors should be removed from (16). Notice that the factors $e^{\gamma u_1}$ have been introduced in (16) so as to include possible u_1 dependence other than the factor $\xi(u_1)(s_1/s_{10})^{\alpha(u_1)}$. This extra dependence is suggested by two-body Regge-pole phenomenology (for the end vertex) as well as by possible dependence arising from the center vertex. The choices of $\gamma_N, \gamma_{\Delta}, s_n (\equiv s_{n0}), s_{\Delta} (\equiv s_{\Delta 0})$, and the nonsense wrong-signature zeros will be discussed separately in more detail as we proceed.

Finally, the values of N_j remain to be specified. If the functional dependences of $\beta_2(u_2)$ and $\beta_j(u_1)$ are given, N_j can be determined by matching the corresponding elementary pole calculations at $\alpha_N = \frac{1}{2}$ ($u_1 = m_N^2$) and $\alpha_{\Delta} = \frac{3}{2}$ ($u_1, u_2 = m_{\Delta}^2$). Or we can determine them by fitting the theoretical results to the experimental data at given values of s, s_1 , and u_2 .

Here we are interested in the Chew-Low plot of $R(s, s_1, u_2)$ obtained by integrating over s_2 and u_1 . A typical integration region is shown in Fig. 3. For small s_1 and $|u_2|$, small s_2 and large negative u_1 are

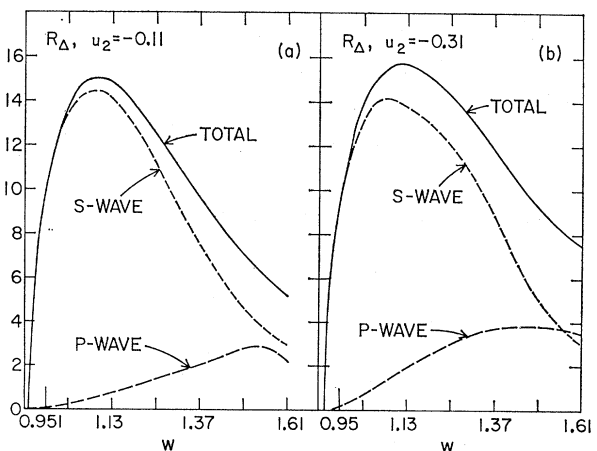


FIG. 5. The R_{Δ} distribution with parameters listed in (17). (a) $u_2 = -0.11$ GeV²; (b) $u_2 = -0.31$ GeV².

not in the integration region, so no cut in u_1 or s_2 is needed in our parametrization.¹⁹

In the following, we discuss separately R_N , R_Δ , and $R_{N\Delta}$, which denote the respective contributions to R from the set of exchanges $(\alpha_\Delta, \alpha_N)$, $(\alpha_\Delta, \alpha_\Delta)$, and their appropriate sum. Within our model, Eqs. (11)–(16), the parameters are varied in many ways. We also discuss the (total) s dependence of $R(s, s_1, u_2)$, the isospin complications, and the “partial-wave” projections. Details of the calculations are not given here. Only some typical results are presented.

A. Enhancement in $\pi\rho$ System

1. s_1 Spectrum (Peak and Width)

We begin with the following parameters¹⁰:

$$\begin{aligned} \alpha_N &= -0.38 + 1.0u, & s_N &= 1, & \gamma_N &= 0, \\ \alpha_\Delta &= 0.15 + 0.9u, & s_\Delta &= 1, & \gamma_\Delta &= 0, \end{aligned} \quad (17)$$

and we assume that the residue functions have zeros at $\alpha_\Delta = -\frac{3}{2}$ and $\alpha_N = -\frac{1}{2}$. The results for $R(s, s_1, u_2)$ are plotted in Figs. 4 and 5. For fixed s [e.g., $s = 31$ (GeV/c)²], and small $|u_2|$ [e.g., $u_2 = -0.11$ (GeV/c)²], R_N alone produces an enhancement at w_R (the peak position) ≈ 960 MeV with $\Gamma_R \approx 80$ MeV; R_Δ alone produces an enhancement at $w_R \approx 1100$ MeV with $\Gamma_R \approx 500$ MeV. In general, we find that an increase of s_N (s_Δ) or decrease of γ_N (γ_Δ) pushes w_R to a larger value and at the same time increases Γ_R .

If we replace $\alpha_\Delta(u_1) + \frac{3}{2}$ or $\alpha_N(u_1) + \frac{1}{2}$ in (16) by a constant, the essential features remain unchanged. This is because only minor contributions come from the large-negative- u_1 region.¹⁹ Even if we replace the whole factor $\beta_j(u_1)\xi(u_1)$ by $1/(u_1 - m_j^2)$ or by a constant, a broad peak still occurs (e.g., $\Gamma_R \gtrsim 550$ MeV) in R_Δ . As far as w_R and Γ_R are concerned, the occurrence of a broad peak is somewhat independent of our choice of $\beta_j(u_1)\xi(u_1)$.

Complications do arise from the behavior of the β_Δ at $\alpha_\Delta = \frac{1}{2}$. A factor $(\alpha_\Delta - \frac{1}{2})$ multiplying β_Δ gives a valley near 1070 MeV. An enhancement in this region is possible only if $\beta_\Delta \neq 0$ at $\alpha_\Delta = \frac{1}{2}$.²⁰

With reasonable values for s_N , s_Δ , γ_N , and γ_Δ , we have varied $\alpha^{(0)}$ and $\alpha^{(2)}$ over a wide range. Again no drastic changes occur. We may conclude that enhancement ($\Gamma_R < 120$ MeV) at $w_R \sim 1070$ MeV is difficult to produce in our model.

¹⁹ Here very little contribution comes from the large-negative- u_1 region. Even neglecting the region $|u_1| < 0.15$ in the integration does not change our results (for small s_1) appreciably.

²⁰ A factor $\alpha_\Delta(u_1) - \frac{1}{2}$ in $\beta_\Delta(u_1)$ will suppress most of the phase-space contribution near $u_1 \approx 0.3$, and therefore for w near 1070 MeV [see Fig. 3(a)].

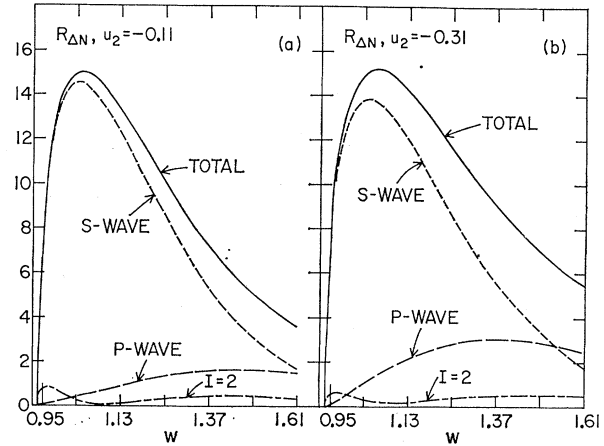


FIG. 6. The $R_{N\Delta}$ distribution for (a) $u_2 = -0.11$ GeV^2 and (b) $u_2 = -0.31$ GeV^2 . The choice of parameters is given by (17). The relations between the amplitudes are $A(I=2) \propto A_\Delta + \eta e^{i\phi} A_N$, $A(I=1) \propto (5/\sqrt{3})(A_\Delta - \frac{1}{3}\eta e^{i\phi} A_N)$, where $\eta = 2$ and $\phi = -3\pi/4$. The full, short-dashed, and long-dashed curves are for the $(\pi\rho)I=1$ system. The dot-dashed curves are for the $(\pi\rho)I=2$ system.

2. u_2 Dependence

For convenience, let us define

$$b(w) = d/du_2 [\ln R(s, s_1, u_2)]_{u_2 \rightarrow 0}, \quad w = (s_1)^{1/2}. \quad (18)$$

Then for small $|u_2|$, $d\sigma_3/ds_1 du_2$ can be described by its associated two-body reaction multiplied by the factor $\exp[b(w)u_2]$. For R_N or R_Δ in the region $w < w_R$, $b(w)$ is positive but small (e.g., $\lesssim 0.5$ GeV^{-2}). For $w > w_R$, $b(w)$ becomes negative. It is too small according to the experimental data. Notice that an extra u_2 dependence, arising from the center vertex, cannot be excluded. If this dependence is weak, however, it is unlikely that any variations of the parameters can produce a factor $b(w_R) > 4$ GeV^{-2} as needed to fit the experimental data.

Other choices of $s_1 \dots$ for (5) and (9) have also been investigated. Although the s_1 spectra are more or less the same, $b(w)$ is then even smaller than the previous results.

B. “Absence” of $I=2$ $\pi\rho$ State and Interference between R_N and R_Δ

Since there are no compelling reasons for either R_N or R_Δ to be dominant, we have to consider them simultaneously in the diagram of Fig. 2(a). By isospin crossing relations,²¹ R_Δ contributes mainly to $(\pi\rho)_{I=1}$.

²¹ As far as isospin is concerned, we treat $\alpha_3^{++}(u_2)$ as an external particle with isospin $\frac{3}{2}$. Then we can relate the isospin states of the final $\pi\rho$ system to the isospin of $\alpha_1(u_1)$ through isospin crossing relations. They are $|(\pi\rho)I=1\rangle = \frac{1}{3}|I_u=\frac{3}{2}\rangle + \frac{2}{3}(10)^{1/2}|I_u=\frac{3}{2}\rangle$, $|(\pi\rho)I=2\rangle = (\frac{2}{3})^{1/2}|I_u=\frac{3}{2}\rangle - (2/15)^{1/2}|I_u=\frac{3}{2}\rangle$, which can be found in, for example, P. Carruthers and J. P. Krisch, Ann. Phys. (N.Y.) **33**, 1 (1965).

For R_N , the situation is reversed. The absence of the exotic $(\pi\rho)_{I=2}$ state in Fig. 2(a) requires a destructive interference between R_Δ and R_N . This enables us to determine approximately their relative weight, and therefore only an over-all normalization is undetermined. In Fig. 6, we plot a typical example of $R(s, s_1, u_2)$ for both $I=1$ and $I=2$ states. Our optional choice of parameters (see the caption of Fig. 6) results in a suppressed $I=2$ state ($<10\%$) for the case of Fig. 2(a). With respect to the case of Fig. 2(b), R_Δ being alone, we have a 12% contribution for $I=2$.²¹ Since we only consider the leading contributions, a small $I=2$ component is acceptable.

Moreover, our predicted cross sections for $\rho^-\pi^0$ [Fig. 2(a)] and $\rho^0\pi^-$ [Fig. 2(b)] are not necessarily equal.²¹ The above choice leads to $\sigma(\rho^-\pi^0)/\sigma(\rho^0\pi^-)\approx 0.6$, which is to be compared with $\sigma(\rho^-\pi^0)/\sigma(\rho^0\pi^-)=1$ when $\pi\rho$ comes from the decay of an $I=1$ resonance. The absence of $(\pi\rho)_{I=2}$, and the branching ratio of $\rho^-\pi^0$ and $\rho^0\pi^-$, will lead to stringent constraints on more detailed future calculations.

C. S Dependence

The function $R(s, s_1, u_2)$ is extremely insensitive to the value of the total energy s .¹⁴ For instance, a change of s from 16 to 10^4 GeV² produces a less than 1% variation in $R(s, s_1, u_2)$, for, say, $s_1 \lesssim 3$ GeV² and $|u_2| \leq 0.5$ GeV². Hence our simple production differential cross section (1) has an energy dependence quite similar to that for the associated two-body reactions at the same total energy. We conclude that if the present model is able to account for the backward A_1 production, then the reaction (14) will possess the same energy dependence as that of reaction (9). We cannot expect A_1^- to be either suppressed or enhanced relative to ρ^- at very high energies.

Experimentally, A_1 seems to have been observed more prominently at 16 GeV/ c than at 8 GeV/ c . A possible explanation is that the background contribution is more important at 8 GeV/ c than at 16 GeV/ c . Detailed identification of the missing mass spectrum X^- in terms of final states is also needed.

D. "Partial-Wave" Analysis of " $\pi\rho$ " System

A rigorous treatment of the various partial waves of the $\pi\rho$ system is by no means trivial.²² Difficulties and complications arise from the facts that the external particles have spins and that, in the present model, one of the incoming particles from which the $\pi\rho$ system emerges is an off-spin-shell Reggeon, i.e.,

the Δ trajectory. In the spirit of our approximation and in view of the impossibility of decomposing the present experimental data into the various helicity amplitudes, we hope to explore roughly the angular momentum structure of the $\pi\rho$ system by making a partial-wave analysis of the spin-averaged amplitude. In other words, to do the partial-wave analysis, we ignore the spin of ρ and treat the $\pi\rho$ system as if it were resulting from a collision of spinless particles. With this understanding, we project the "partial waves" of the $\pi\rho$ system for all the three cases R_N , R_Δ , and $R_{N\Delta}$.

We found that for $w \lesssim w_R$ and $|u_2| \lesssim 0.3$ GeV², $R(s, s_1, u_2)$ and hence $d\sigma_3/ds_1 du_2$ are predominantly "S wave" (about 90%). When w increases beyond 1.25 GeV, the "P wave" becomes more important and eventually dominates, yet the enhancement is much smaller than that for the S wave occurring at lower w . In general, the peak of the S wave (P wave) occurs at lower (higher) w , and the width is smaller (bigger) than that of the total amplitude. These features can be understood from the centrifugal-barrier effects. The contributions of the "S and P partial waves" of R_N , R_Δ , and $R_{N\Delta}$ are plotted in Figs. 4, 5, and 6, respectively. Under variations of the parameters, the shapes of the S-wave and P-wave projections are mostly stable, but their relative abundance and u_2 dependence vary moderately.

IV. COMPARISON WITH FORWARD A_1 PRODUCTION

In this section we discuss briefly two forward A_1 production processes for comparison with the backward case. The first one contains a diffraction vertex, the second does not.

$p\pi \rightarrow \rho(\pi\rho)$.⁴ Here the set (α_P, α_π) is the leading contribution, where α_P and α_π are the Pomanchukon and pion trajectories.²³ We have varied the intercepts and slopes of α_P and α_π . It is interesting to note that with a wide range of the parameter values,²⁴ e.g., $0.5 \lesssim \alpha_P^{(0)} \leq 1$, $0 \lesssim \alpha_P^{(2)} \lesssim 0.5$, $-0.5 \leq \alpha_\pi^{(0)} \lesssim 0$, and $0.5 \lesssim \alpha_\pi^{(2)} \lesssim 1$, features similar to the backward cases are observed: $(w_R, \Gamma_R) \approx (1040 \text{ MeV}, 450 \text{ MeV})$. They are mainly "S wave" (see Sec. III D). The analogous quantity R of the present case, where the associated two-body reaction is the elastic $\pi\rho$ scattering, is also extremely insensitive to the total energy s . Let us emphasize that even though a considerable slope for the pion trajectory is necessary,⁴ i.e., the pion has to be Reggeized in order to produce such a narrow enhancement (full width ~ 450 MeV), the exact values of the slopes of α_P and α_π and the difference of their

²² We refer the reader to the following articles on the subject of partial-wave analysis of a two-particle subchannel of the final state in 2-body \rightarrow 3-body reactions: L. Resnick, Phys. Rev. **150**, 1292 (1966); **175**, 2185 (1968); J. G. Rushbrooke, *ibid.* **177**, 2357 (1969); C. D. Froggatt and G. Ranft, Phys. Rev. Letters **23**, 943 (1969).

²³ Here (α_P, α_ρ) is also allowed. For simplicity we have omitted such contributions in our calculation.

²⁴ We vary the value of $\alpha_P^{(0)}$ for the purpose of indicating that the shape of R is not very sensitive to it. For constant asymptotic total cross sections of two-body scatterings, we need, of course, $\alpha_P^{(0)}=1$.

intercepts are not very crucial. This has already been demonstrated in the case of backward scattering discussed in Sec. III.

$nK^- \rightarrow \Lambda(\pi\rho)^-$. As an example, (α_{K^*}, α_K) is used. With a reasonable choice of parameters [viz., $\alpha_{K^*} = 1 + (t - m_{K^*}^2)$ and $\alpha_K = t - m_K^2$, where t is the forward momentum transfer squared], an enhancement occurs near $w = 1040$ MeV with $\Gamma_R \approx 400$ MeV and $b(w_R) \approx 2$. These are similar to the results of the previous case where α_P is allowed. Strictly speaking, isospin complications have to be considered but no change in the main feature is expected. In this case the dynamic behavior of the amplitude is analogous to that of the backward scattering, but kinematics may introduce differences.

In forward scattering for small s_1 , an increase in $|t_2|$ (the variable analogous to $|u_2|$) in the region $t_2 < 0$ pushes the phase space quickly away from the nearby pole [see Fig. 3(b)]. This feature coupled with the peripheral nature of the Regge amplitude makes $b(w_R)$ large. However, in the backward case, when $|u_2|$ increases, the upper boundary of the (s_2, u_1) phase space moves very little [see Fig. 3(a)]. Therefore $b(w_R)$ is smaller than that of the forward case, in the absence of strong center-vertex u_2 dependence.

V. CONCLUSION

As we have discussed in the previous sections, the double-Regge-pole model can generate a mass enhancement in the final $\pi\rho$ system of reaction (14). The peak is at about 1040 MeV and the width is 450 MeV. This result is analogous to the forward cases. For both backward and forward reactions, the enhancements arise from the interplay between the peripheral nature of the DR amplitudes and the threshold behavior of the phase-space kinematics. The essential features of the Chew-Low plots for the $R(s, s_1, u_2)$ spectra are insensitive to variations of the trajectory and other parameters. Concerning the u_2 dependence, we found that it is impossible to reproduce the sharp (backward) peripheral behavior of

A_1 production. To accommodate this behavior, a form factor which may come from the center vertex is required. Information about other variables (e.g., the Treiman-Yang angle, etc.) is necessary in order to further pin down this dependence.

In backward scattering, unlike the forward case involving a diffraction vertex, both isospins 1 and 2 can be present in the $\pi\rho$ system. We have demonstrated that the exotic $I=2$ channel can be suppressed relative to the $I=1$ channel.

With the over-all normalization constants N_j yet to be fixed, one cannot rule out the possibility that the DHD or DR model accounts only for the background on which the true A_1 resonance is superimposed. This, of course, contradicts the duality principle and raises the problem of double counting. Under such circumstances, the structure of the background would be more complicated than what is usually expected for reactions not involving (virtual) diffractive vertices.

Even with the assumption of duality for the backward reactions, the DR model can only dictate an averaged behavior of A_1 . Its detailed features (i.e., the resonance height, width, and u dependence) are hard to reproduce. Therefore, if A_1 is consistently observed in various reactions as a narrow-mass enhancement, it would be more convenient to describe it as a genuine resonance.

In order to further establish the role of the duality principle in backward production processes like (14), more efficacious models like the five-point Veneziano functions should be pursued.²⁵ The complications of isospin and spin have to be incorporated properly into the model.

ACKNOWLEDGMENTS

We wish to thank Dr. R. F. Peierls, Dr. K. W. Lai, Dr. H. R. Blieden, and Dr. D. Garelick for helpful discussions, and Dr. R. W. Brown for reading the manuscript.

²⁵ K. Bardakci and H. Ruegg, Phys. Letters **28B**, 342 (1968).